

STATISTICS, MORPHOLOGY, AND ENERGETICS OF ELLERMAN BOMBS

Manolis K. Georgoulis¹, David M. Rust¹, Pietro N. Bernasconi¹, and Brigitte Schmieder²

¹*The Johns Hopkins University Applied Physics Laboratory, 11100 Johns Hopkins Rd., Laurel, MD 20723, USA*

²*Observatoire de Paris, Section Meudon, 92195 Meudon Principal Cedex, France*

ABSTRACT

We have performed a detailed analysis of several hundreds $H\alpha$ Ellerman bombs in the low chromosphere, above an emerging flux region. We find that Ellerman bombs may be small-scale, low-altitude, magnetic reconnection events that heat the low chromosphere in the active region. Their energy content varies between 10^{27} *erg* and 10^{28} *erg*, typical of sub-flaring activity.

Key words: Chromosphere; Ellerman bombs; Magnetic fields; Photosphere.

1. INTRODUCTION

Ellerman bombs (EBs), or chromospheric “moustaches”, are small-scale, short-lived (10 – 20 *min*) brightenings, seen mostly at the wings of the $H\alpha$ line. They are not detectable at the $H\alpha$ line center, which implies that they are features of the upper photosphere (Severny 1968), or the low chromosphere (Payne 1993). EBs correlate with a variety of other features, such as $H\alpha$ surges (Rust 1968), facular granules (Dara et al. 1997), and moving magnetic features (Nindos & Zirin 1998). EBs are also seen in wavelengths other than $H\alpha$, such as the ultraviolet (UV) continuum emission at 1600 Å (Qiu et al. 2000). This emission originates from the temperature minimum (T_{min}) region and suggests that EBs have a typical vertical extent of the order of one, to a few, hundred *km*.

EBs are typical features of dynamic, emerging flux regions (EFRs). They occur and recur in swarms above strong (≥ 500 G) photospheric magnetic fields. Whether EBs occur above unipolar, or bipolar, fields, is a highly debated issue. Early authors asserted that EBs are sub-flares, related to low-altitude magnetic reconnection (see, e.g., Severny 1964). This is also a subject of debate, on the grounds of several arguments (Payne 1993). Despite numerous attempts, the triggering mechanism of EBs remains elusive.

Georgoulis et al. (2002), hereafter Paper I, performed a detailed analysis of the EBs observed by the balloon-borne Flare Genesis Experiment (FGE; Rust 1994a). The FGE data revealed hundreds of EBs within ~ 3.5 *hr*. The target was the EFR NOAA 8844. The data set is briefly described in §2. Sections §3, §4, and §5 describe aspects of the analysis. In §6 we offer an interpretation of EBs. In §7 we outline our conclusions.

2. OBSERVATIONS AND DATA REDUCTION

The FGE circumnavigated Antarctica for 17 *d* in January, 2000. The instrumentation is described in detail by Rust (1994b), and Bernasconi et al. (2000). Early on January 25, EFR NOAA 8844 showed signs of rapid development. The FGE recorded 55 high-resolution (0.5'') vector magnetograms of the active region (AR), with a cadence ~ 3.5 *min*. Magnetograms were obtained at the photospheric line Ca I (6122.2 Å). Simultaneous observations at both wings of the Ca I line gave 28 Dopplergrams (0.8''), with a cadence ~ 7.5 *min*. Also acquired, were 28 off-band $H\alpha$ filtergrams, obtained at $H\alpha - 0.8$ Å, with a resolution $\sim 0.8''$ and a cadence ~ 7.5 *min*.

The FGE data were complemented by data from the Transition Region And Coronal Explorer (TRACE). TRACE data consisted of 16 UV 1600 Å filtergrams of the T_{min} region above the EFR. Moreover, a correlation tracking algorithm, applied on the FGE continuum images, provided the horizontal, photospheric flow pattern (proper motions), with a resolution $\sim 4'' - 6''$.

Figure 1a shows a typical line-of-sight (LOS) longitudinal magnetogram of the AR NOAA 8844. The corresponding $H\alpha$ filtergram is given in Figure 1b. AR NOAA 8844 consisted of a pair of small sunspots, with the follower spot adjacent to a small supergranular cell (Area 1). Intense, systematic, spotward flows were seen. At the same time, several EBs were flickering above the AR (Figure 1b).

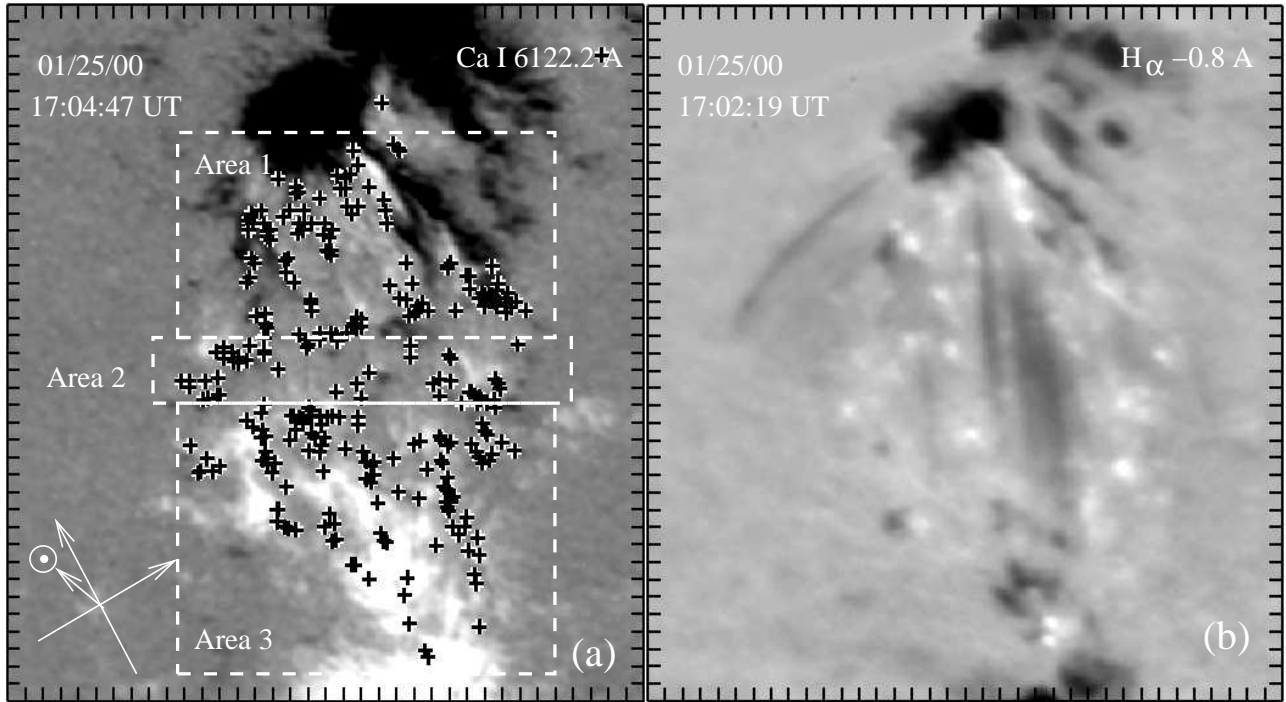


Figure 1. Views of the EFR NOAA 8844: (a) LOS longitudinal magnetogram. The mean origin locations of 295 EBs are shown with crosses. The orientation of the AR and the location of the disk center are given on the bottom left corner. (b) $H\alpha$ -0.8 Å filtergram. The brightenings correspond to EBs. Tic mark separation in both images is 2''.

3. THE MORPHOLOGY OF EBs

In Figure 1a we show the mean origin locations of 295 EBs (crosses). These EBs were identified using a contrast threshold 0.08, close to the average EB contrast. For a total EB-producing area of $\sim 1800 \text{ arcsec}^2$, we find a mean occurrence rate $\sim 1.43 \text{ EBs min}^{-1}$. EBs occur and recur in the following areas:

- (1) On the supergranular boundary (strong, bipolar fields), and in the interior of the supergranule (Area 1). In the latter case, EBs are associated with moving dipolar features (MDFs; Bernasconi et al. 2002)
- (2) In the polarity reversal area (Area 2), where EBs are associated with weaker, but still bipolar, fields.
- (3) At the vicinity of the leading spot (Area 3). This area shows strong, plage-like magnetic fields, but no neutral lines (unipolar fields).

Therefore, we find that EBs can occur above both unipolar and bipolar magnetic fields.

The typical size of EBs is $\sim 1.8'' \times 1.1''$, comparable to our spatial resolution. We have also found indications of much smaller EBs. Therefore, several EBs may remain undetected. EBs are elongated structures with a preferential degree of elongation $\sim 40\%$,

that is, a length 40% larger than their width. Other morphological properties of EBs include the following:

- (1) EBs are associated with photospheric descending motions. This implies that EBs are located close to the footpoints of newly emerged flux tubes, where drainage of cold, field-free plasma back to the photosphere accounts for the downflows.
- (2) The EB loci follow the photospheric proper motions, especially in areas of systematic flows.
- (3) EBs are associated with UV 1600 Å bright points. The brighter the EBs, the higher the percentage of association. For conspicuous EBs, this percentage reaches $\sim 90\%$.

The morphological properties of EBs are summarized in Table 1.

4. THE STATISTICAL PROPERTIES OF EBs

We have found (Paper I) that the clusters of EBs are fractal structures. The mean fractal dimension is ~ 1.4 . This suggests an intrinsic self-similarity in the clustering process of EBs.

Self-similarity is also revealed from several EB “size” parameters, such as the duration, the spatial coverage, the peak activity, and the total activity of EBs.

